The Astrophysical Journal, 608:1124–1132, 2004 June 20

FILAMENT OSCILLATIONS AND MORETON WAVES ASSOCIATED WITH EIT WAVES

Takenori J. Okamoto, Hidekazu Nakai, and Atsushi Keiyama
Department of Astronomy, Kyoto University, Sakyo-ku, Kyoto 606-8502, Japan; okamoto@kwasan.kyoto-u.ac.jp

and

Noriyuki Narukage, Satoru UeNo, Reizaburo Kitai, Hiroki Kurokawa, and Kazunari Shibata
Kwasan and Hida Observatories, Kyoto University, Yamashina-ku, Kyoto 607-8417, Japan
Received 2003 October 17; accepted 2004 March 4

ABSTRACT

In this paper we compare EUV Imaging Telescope (EIT) waves with simultaneous phenomena seen in Hα in order to address the question of what an EIT wave is. We surveyed the events associated with solar flares larger than *GOES* M-class in 1999–2002. The Hα data are taken with the Flare-monitoring Telescope (FMT) at the Hida Observatory of Kyoto University. Among 14 simultaneous observations of EIT waves and Hα, 11 were found to have filament eruptions, three were associated with Moreton waves, and one was found to have only filament oscillations. This shows that we cannot see clear wave fronts in Hα even if EIT waves exist, but that it is possible to recognize invisible waves by means of filament oscillations. The nature of filament oscillations and Moreton waves associated with EIT waves is examined in detail, and it is found that the filament oscillations were caused by EIT waves.

Subject headings: shock waves — Sun: corona — Sun: filaments — Sun: flares — Sun: oscillations

1. INTRODUCTION

In 1960, Moreton reported a flare-associated wave seen in Hα that propagated on the chromosphere. These waves, which are called Moreton waves, are directional, and their speeds are 330–4200 km s^{-1} (Smith & Harvey 1971). Uchida (1968) established that they are a chromospheric manifestation of MHD fast-mode shocks propagating in the corona. Now, this model is widely accepted. When *Yohkoh* was launched in 1991, it was expected that the coronal counterpart of a Moreton wave would be found. However, such a wave was not observed. Thompson et al. (1999) reported the discovery of a flare-associated wave propagating in the corona with the EUV Imaging Telescope (EIT; Delaboudinière et al. 1995) aboard the *Solar and Heliospheric Observatory* (*SOHO*). These waves were named "EIT waves." A large number of EIT waves have been observed and studied. Many EIT waves have been found to be associated with coronal mass ejections (CMEs) and type II radio bursts (Biesecker et al. 2002). However, almost all the EIT-wave speeds are one-half or one-third of the Moreton-wave speeds. Moreover, an EIT wave usually spreads from a flare site isotropically, while a Moreton wave propagates within a somewhat finite solid angle. In a simultaneous observation, it was shown that an EIT wave and a Moreton wave are different waves, because the EIT wave front did not correspond to that of the Moreton wave, and also, their speeds were very different (Eto et al. 2002). On the other hand, Warmuth et al. (2001) suggested that an EIT wave is a decelerated Moreton wave. Hence, it is difficult to conclude whether EIT waves are the coronal counterpart of Moreton waves or not, and the question of what an EIT wave is has not been solved.

Recently, the Soft X-Ray Telescope (SXT; Tsuneta et al. 1991) on board *Yohkoh* discovered wavelike disturbances in the solar corona associated with flares (Khan & Hudson 2000; Hudson et al. 2003), which are called "X-ray waves." Simultaneous observations of a Moreton wave and an X-ray wave were reported by Khan & Aurass (2002) and Narukage et al. (2002). They suggest that X-ray waves are coronal counterparts of Moreton waves. Vršnak et al. (2002) reported flare waves in the absorption line of He I at 10830 Å, which are links between Hα Moreton and EIT waves.

It should be noted that a Moreton wave often triggers a filament oscillation, or a winking filament (Smith & Ramsey 1964). This is a phenomenon in which a filament disappears and reappears repeatedly at a specific wavelength, since it moves first to the red wing and then to the blue wing when a Moreton wave hits it. It has been reported that even when Moreton waves are not clearly seen, filament oscillations are observed. Hence, the observation of such a winking filament teaches us the existence of an invisible Moreton wave (Smith & Ramsey 1964; Ramsey & Smith 1965; Smith & Harvey 1971; Eto et al. 2002).

The purpose of this paper is to see what happened in Hα when an EIT wave is generated. We searched for EIT waves by surveying the events associated with solar flares larger than *GOES* M-class in 1999–2002 and compared EIT waves with simultaneous phenomena seen in Hα that were taken with the Flare-monitoring Telescope (FMT; Kurokawa et al. 1995) at the Hida Observatory. As a result of this survey, we found 14 EIT events that were observed simultaneously with Hα, and among them, 11 were found to have filament eruptions, three were associated with Moreton waves, and one was found to have only filament oscillations. In this paper, we mainly focus on filament oscillations and Moreton waves associated with EIT waves. We determine whether an EIT wave can produce filament oscillations in the same way that Moreton waves can.

2. OBSERVATION

The EUV images were observed with the EIT on board *SOHO*. The observation in the present study was made in a wavelength range centered on 195 Å, comprising an Fe XII line emitted at 1.2×10^6 K at typical coronal density. The time resolution was about 12 minutes.

The images in Hα were taken with FMT at Hida Observatory of Kyoto University. The FMT observes four full-disk

TABLE 1
EIT Waves and the Other Phenomena

Day	Start[a]	End[b]	*GOES* Class	Wave/Burst Speed (km s^{-1})				Filament Eruption (km s^{-1})	Reference
				EIT	Moreton	Type II	CME		
2000 Mar 3	02:18	02:22	M3.8	450	1050	1280	841	941	Narukage et al. 2002
2000 Jun 15	23:36	23:49	M2.0	360	397	...	658	152	Fig. 1
2000 Jul 18	04:59	05:38	M1.9	270	...	1040	...	473	
2000 Nov 23	23:18	23:37	M1.0	180	...	468	690	58	
2000 Nov 24	04:55	05:08	X2.0	260	...	519	994	610	
2000 Nov 25	00:59	02:01	M8.2	130	...	1216	2519	117	
2001 Apr 10.....	05:06	05:42	X2.3	370	...	2062	2411	304	Filament oscillations (Fig. 7)
2001 May 20.....	06:00	06:06	M6.4	310	...	824	546	215	
2001 Nov 22	22:32	24:06	M9.9	290	...	...	1437	28	
2002 Feb 20.....	05:52	06:16	M5.1	350	...	395	952	910	
2002 Mar 18	02:16	04:00	M1.0	230	...	...	989	...	
2002 Aug 14.....	01:47	02:46	M2.3	160	...	608	1356	...	
2002 Aug 22.....	01:47	02:05	M5.4	280	...	646	1005	640	
2002 Oct 4	22:32	22:51	M2.7	(230)[c]	600	288	...	...	Fig. 3

[a] Start time when *GOES* X-ray flux went over M-class.
[b] End time when *GOES* X-ray flux became under M-class.
[c] On account of poor data, this is an estimated speed of the EIT wave that occurred with the onset of the flare.

images, in Hα center, H$\alpha + 0.8$ Å, H$\alpha - 0.8$ Å, and white light, and one solar-limb image in Hα center. We used three full-disk images, in Hα center, H$\alpha + 0.8$ Å, and H$\alpha - 0.8$ Å. The time cadence is 1 minute. We can find Moreton waves owing to the high time resolution.

Type II radio bursts were recorded with the Hiraiso Radio Spectrograph (HiRAS; Kondo et al. 1995). CMEs were observed with the Large Angle and Spectrometric Coronagraph (LASCO; Brueckner et al. 1995) on board *SOHO*, and we used the *SOHO* LASCO CME catalog.

3. ANALYSIS

We found 33 EIT waves in 358 M- and X-class flares that occurred during daytime observing in Japan (22:00–07:00 UT). Among the 33 EIT waves, 14 events were later found to have been observed with FMT. In these 14 events, we surveyed phenomena in Hα. Moreover, we checked whether 34 EIT-wave events had type II radio bursts and CMEs or not and measured their speeds if they existed. On the basis of the coronal electron density model (Mann et al. 1999), we calculate the velocity and the distance from the photosphere of the type II radio burst. The results are listed in Table 1.

It was found that three events, 2000 March 3, 2000 June 15, and 2002 October 4, had Moreton waves, and one event, 2001 April 10, had no Moreton wave but did display filament oscillations. The event on 2000 March 3 has been already analyzed in detail by Narukage et al. (2002), who reported that an X-ray wave existed and that the wave front corresponded to that of the Moreton wave. Hence, we do not refer to the event. Eleven events show filament eruptions, and one event has a spraylike phenomenon. The filament erupted with high speed (473–941 km s^{-1}) in five events and ejected slowly (58–215 km s^{-1}) in seven events (see Table 1). However, there is no other remarkable phenomenon in all the events. We discuss the other Moreton-wave events, 2000 June 15 and 2002 October 4, and the oscillating filament event on 2001 April 10 in the following subsections.

3.1. *Moreton Waves*

3.1.1. *On 2000 June 15*

The flare associated with the Moreton wave is an M2.0 *GOES* flare on 2000 June 15. The EIT wave was found at 23:47 and 23:59 UT, and the Moreton wave was observed at 23:39 and 23:40 UT. After 23:41 UT, the Moreton wave became invisible. Therefore, the Moreton wave appears in only two frames. Figure 1 shows the FMT images observed in H$\alpha + 0.8$ Å and the relationship between the Moreton wave and the EIT wave. The Moreton wave is shown as intensity images (Fig. 1*b*) and running-difference images (Fig. 1*c*) magnified in the box of Figure 1*d*. Running-difference images show the change between consecutive images by subtracting a previous image from themselves digitally. Figure 1*d* is a cartoon of the Moreton- and EIT-wave fronts. We plot the time evolution of the distances of the Moreton wave and the EIT wave with *GOES* X-ray flux data in Figure 2. The extrapolated start time and the speed of the Moreton wave are 23:37 UT and 397 km s^{-1}, respectively; for the EIT wave, 23:38 UT and 360 km s^{-1}, respectively. Hence, in this case the Moreton wave and the EIT wave may be the same wave.

3.1.2. *On 2002 October 4*

The flare associated with the Moreton wave is an M2.7 *GOES* flare that took place on 2002 October 4. During this event, EIT data are of very poor cadence, and we confirm the EIT wave only with one differential image, at 23:11 UT. On the other hand, the Moreton wave was observed at 22:39, 22:40, and 22:41 UT. After 22:42 UT, the Moreton wave became invisible. Therefore, the number of images of the Moreton wave is only three. Figure 3 shows the FMT images observed in H$\alpha + 0.8$ Å and the relationship between the Moreton wave and the EIT wave. The Moreton-wave images are running-difference images (Fig. 3*a*), running-difference images to enhance the front (Fig. 3*b*), and differential running-difference images for further enhancement (Fig. 3*c*) magnified in the box in Figure 3*e*. Figure 3*e* shows a sketch of the

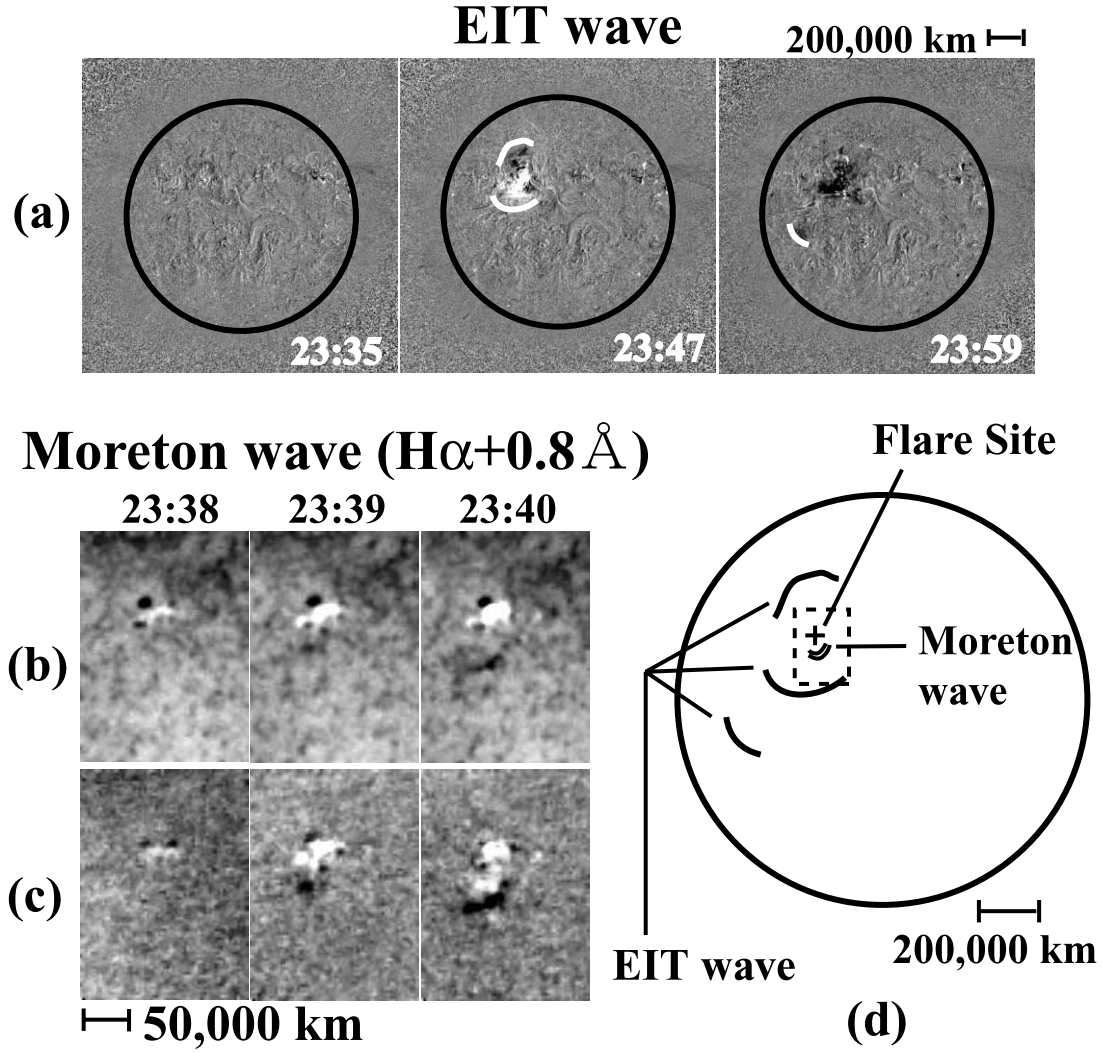

FIG. 1.—Moreton wave observed in Hα + 0.8 Å with the Flare-monitoring Telescope (FMT) at Hida Observatory and an EIT wave observed with *SOHO* EIT at nearly the same time on 2000 June 15. (*a*) Running-difference images of the EIT wave at 23:35, 23:47, and 23:59 UT. (*b*) Original images of the Moreton wave at 23:39 and 23:40 UT. (*c*) Running-difference images of the Moreton wave. (*d*) Wave fronts of the Moreton wave and the EIT wave. The speed of the Moreton wave and the EIT wave is 397 and 360 km s^{-1}, respectively.

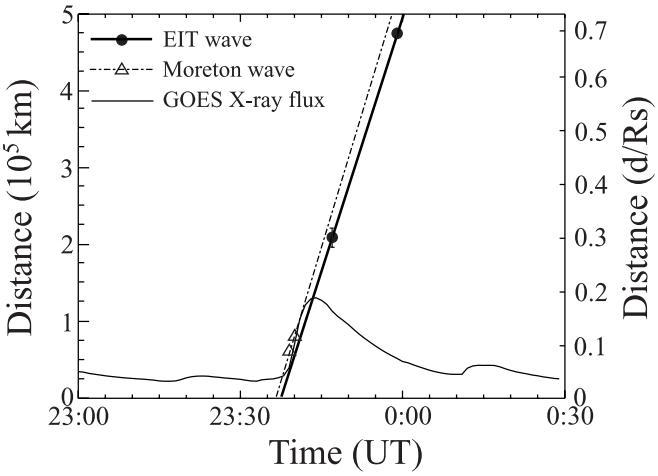

FIG. 2.—Time evolution of the distances of the Moreton EIT waves on 2002 June 15. *GOES* X-ray flux data at the 1–8 Å channel are also shown. The distances from the flare site are plotted for the Moreton wave and the EIT wave. The speeds of the Moreton and EIT waves are 397 and 360 km s^{-1}, respectively. "Rs" represents the solar radius (695,800 km).

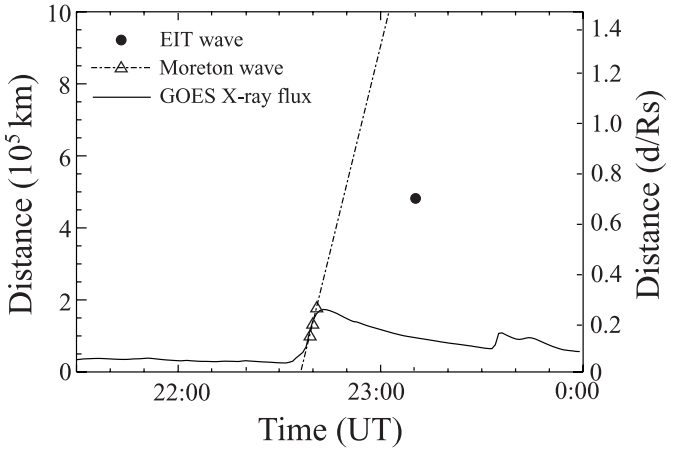

FIG. 4.—Same as Fig. 2, but for 2002 October 4. The speed of the Moreton wave is 600 km s^{-1}.

Moreton- and EIT-wave fronts. We plot the time evolution of the distances of the Moreton and EIT waves with *GOES* X-ray flux data in Figure 4. The extrapolated start time and the speed of the Moreton wave are 22:37 UT and 600 km s^{-1}, respectively. Since the EIT wave was found in only one image, we cannot know the speed. If the EIT wave occurred with the Moreton wave, the speed is 230 km s^{-1}, and this is a typical speed for an EIT wave. The position of the EIT wave is very different from the extrapolated line of the Moreton wave. Therefore, in this case the EIT wave is not the same wave as the Moreton wave.

3.2. *Filament Oscillations*

We analyze this oscillation event in detail and discuss the relationship between oscillations and the EIT wave. The oscillation event is associated with a big two-ribbon flare, *GOES* flare X2.3, which occurred in NOAA Active Region 9415 (S23°, W01°) at 05:10 UT on 2001 April 10. This flare was studied by many authors (Pike & Mason 2002; Asai et al. 2003; Foley et al. 2003). An EIT wave occurred and propagated from 05:11 to 05:35 UT, and four filament oscillations were found. Figure 5 shows a series of running-difference

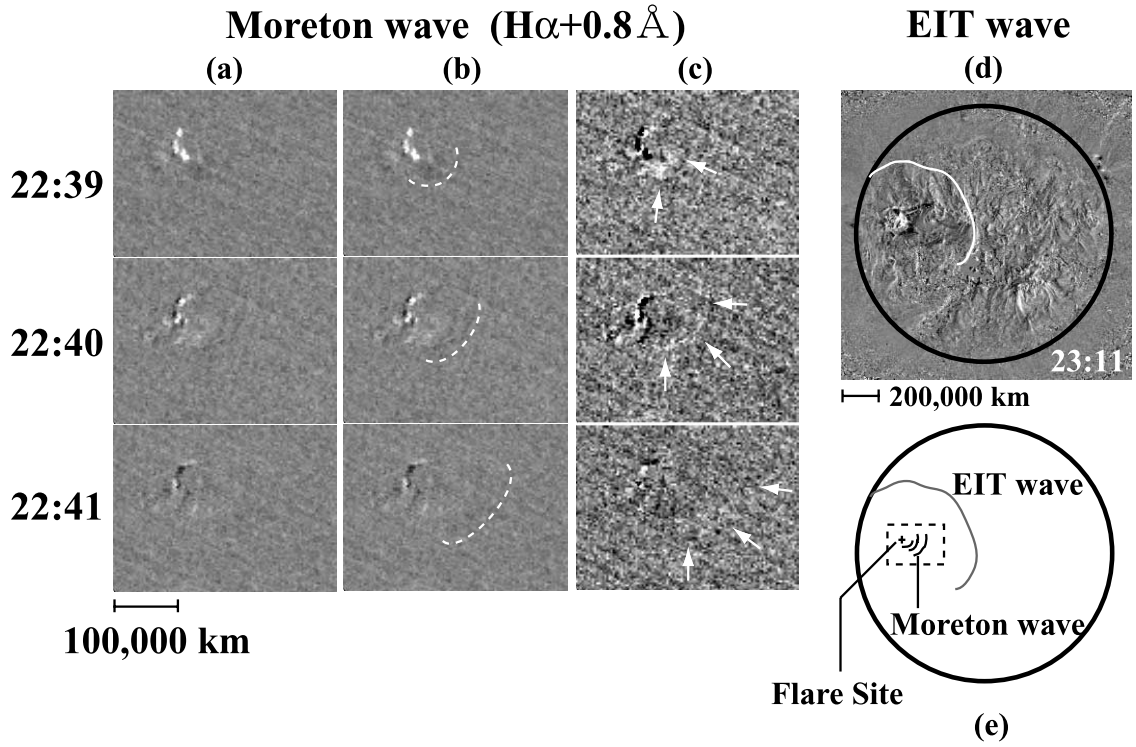

FIG. 3.—Moreton wave observed in Hα + 0.8 Å with FMT at Hida Observatory and an EIT wave observed with *SOHO* EIT at nearly the same time on 2002 October 4. (*a*) Running-difference images of the Moreton wave in the box in (*e*) at 22:39, 22:40, and 22:41 UT. (*b*) The same as (*a*), but with the dashed lines as Moreton-wave fronts. (*c*) Differential running-difference images to emphasize the Moreton wave. (*d*) The white line represents the EIT wave front at 23:11 UT. (*e*) Wave fronts of the Moreton EIT waves. The speed of the Moreton wave is 600 km s^{-1}.

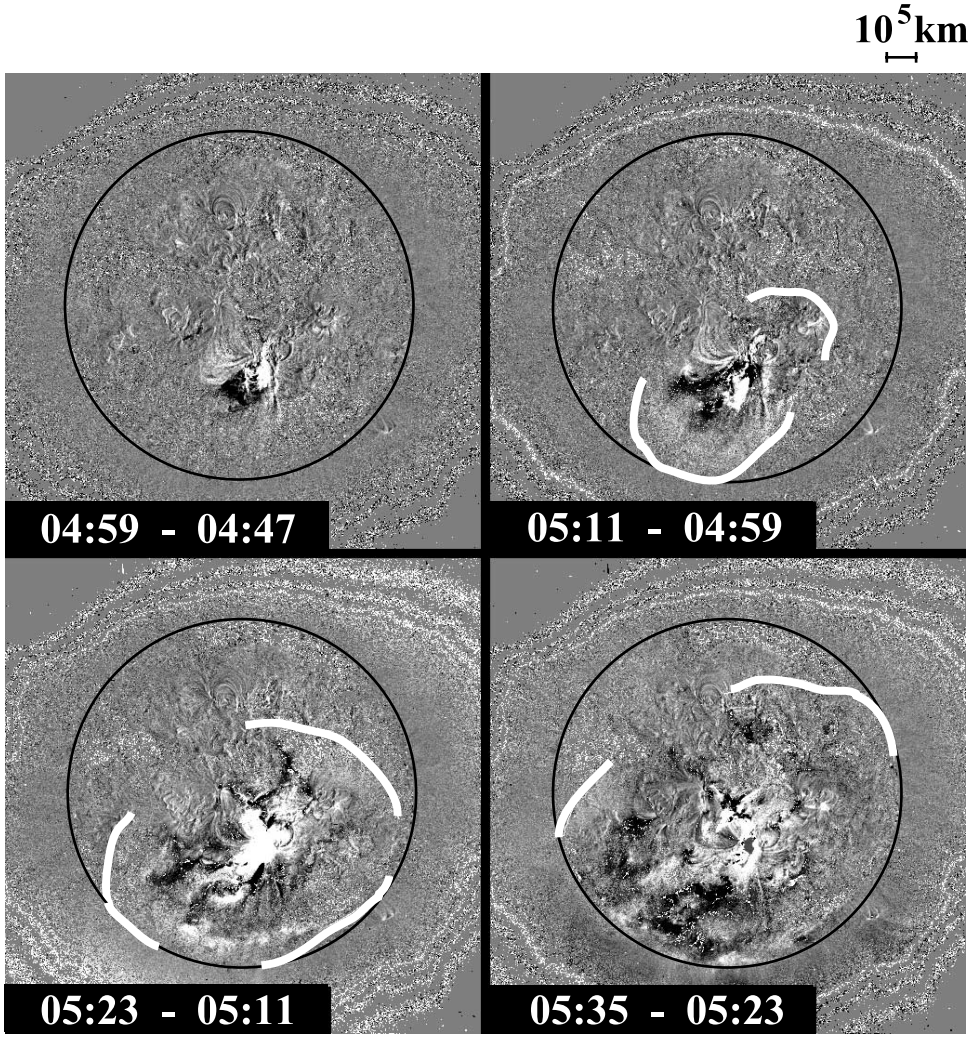

FIG. 5.—*SOHO* EIT 195 Å running-difference images showing the progression of the 2001 April 10 EIT wave. The sequence consists of EIT 195 Å images at 04:59, 05:11, 05:23, and 05:35 UT, with previous images subtracted from them. The black circle represents the solar limb, and the white curves represent EIT-wave fronts.

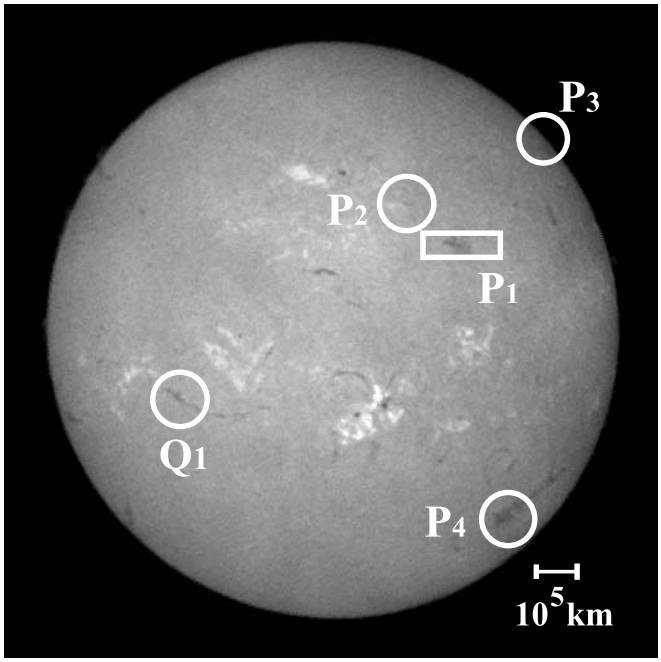

FIG. 6.—Full-Sun Hα (line center) image at 05:00 UT on 2001 April 10, taken with the FMT at Hida Observatory. Box and circles indicate the locations of filament oscillations P1, P2, P3, and P4. Q1 is the location of nonoscillating dark filaments. The field of view of Fig. 7 is box P1.

EIT-wave images at 04:59, 05:11, 05:23, and 05:35 UT. The increase in emission is shown in white, while the decrease in emission is indicated in black. The white lines in Figure 5 represent EIT-wave fronts, and the black circle represents the solar limb. We found that the waves propagated roughly from the flare site in two directions, northward and southward.

We found filament oscillations in four regions, shown in Figure 6. In the figure, we labeled the oscillation regions as P1, P2, P3, and P4. The distances between the flare site and P1, P2, P3, and P4 are 4.7×10^5, 5.2×10^5, 9.5×10^5, and 5.6×10^5 km, respectively. Region P1 was a very clear oscillation. Regions P2 and P3 were small oscillations. Regions P3 and P4 were near the solar limb and a little irregular. Regions P1, P2, and P3 were caused by the northward EIT wave and P4 by the southward one. Thus, we analyzed the two regions separately.

Figure 7 shows FMT images of the oscillating filament at wavelengths of H$\alpha - 0.8$ Å (*left*), Hα center (*middle*), and H$\alpha + 0.8$ Å (*right*). The field of view is indicated by box P1 in Figure 6. The image at 05:00 UT is from before the filament oscillated. A dark region appeared faintly in the red image (we call this "in red") at 05:17 UT. Then at 05:24 UT, it was invisible in red, while it also became faintly visible in blue. Although these are very faint, one can see darkening areas from 05:28 in blue and red clearly. This is the so-called winking filament.

The changes in the emission in three wavelengths of P1 versus time are plotted in Figure 8. The horizontal and vertical axes are time (UT) and ratio of intensity compared with the emission at 05:00 UT in each wavelength, respectively. The data before 05:11 UT were excluded because it was cloudy from 05:04 to 05:11 UT. In red, the emission started to decrease at about 05:23 UT. Simultaneously, the emissions in both blue and center began to increase. Then the emission in blue decreased, while that in red increased. We find that this process repeated 2.5 times in a period of about 70 minutes.

Similarly, the change of emissions in P2 and P3 are shown in Figure 9. Moreover, we checked other dark filaments that did not indicate oscillations in Hα images. One light curve of dark, nonoscillating filaments is shown in Figure 10 (circle Q1 in Fig. 6). This filament has large-amplitude oscillations in all wavelengths, while those in P2 and P3 have a large depression in blue.

Figure 11 shows the time evolution of the distances of the EIT wave, the type II radio burst, and the filaments oscillations with *GOES* X-ray flux data. We plot the distances from the flare site of the EIT wave and the filament oscillations, as well as the distance from the photosphere with coronal electron density model for the type II radio burst. The lines are interpolated and extrapolated for the EIT wave, filaments oscillations, and type II radio burst. The extrapolated start time of the EIT wave and filament oscillations are 04:57 and 04:59 UT, respectively. The speeds of the EIT wave and the propagating wave that caused filament oscillations are 370 and 330 km s^{-1}, respectively. Judging from this result, we consider the EIT wave to have caused filament oscillations directly.

Although a Moreton wave was not observed in this event, a type II radio burst was observed by the HiRAS. According to the MHD fast-mode shock-wave model (Uchida 1974), a part on the chromosphere depressed by a shock-wave front is a Moreton wave, while a type II radio burst is the upward shock-wave front. Thus, their speeds should be comparable. In this event, the speed of the type II radio burst is 2062 km s^{-1} and the extrapolated start time is 05:12 UT. Both the start time and speed of the type II radio burst are very different from those of the EIT wave. Therefore, we do not think that this EIT wave is a shock wave corresponding to a type II radio burst.

We are certain that the filament oscillations were caused only by the EIT wave, since there is no Moreton wave.

For region P4, associated with the southward EIT wave, the changes in the emission in three wavelengths of P4 versus time are plotted in Figure 12. The emission in blue started to decrease at 05:20 UT, and then periodic fluctuation is seen.

We plot the time evolution of the distances of the EIT wave, the type II radio burst, and the filaments oscillations with *GOES* X-ray flux data in Figure 12, as well as in Figure 11. The extrapolated start time and the speed of the EIT wave are 04:48 UT and 285 km s^{-1}, respectively. The start time of the southward EIT wave is earlier by 9 minutes than that of the northward one. This is why the distance of the EIT wave is smaller at 05:23 UT: the EIT wave was decelerated or interrupted by the dark filament at P4. Moreover, the distance of the EIT wave from the filament cannot be measured, since the EIT wave passed across the solar limb. This oscillation is all we found in the south region of the flare site, and thus it is difficult to determine whether its cause is the EIT wave or the type II radio burst.

4. DISCUSSION

We surveyed events in Hα associated with EIT waves and found three Moreton-wave events and one oscillating filament event. Three out of 14 Hα events associated with large flares, or 21%, are related to Moreton waves.

All these EIT waves are diffuse waves. Thompson et al. (2000) and Warmuth et al. (2001) suggested that diffuse EIT waves are decelerated Moreton waves, while Eto et al. (2002) reported that some EIT waves are not coronal counterparts of Moreton waves. As for our Moreton-wave events, the EIT

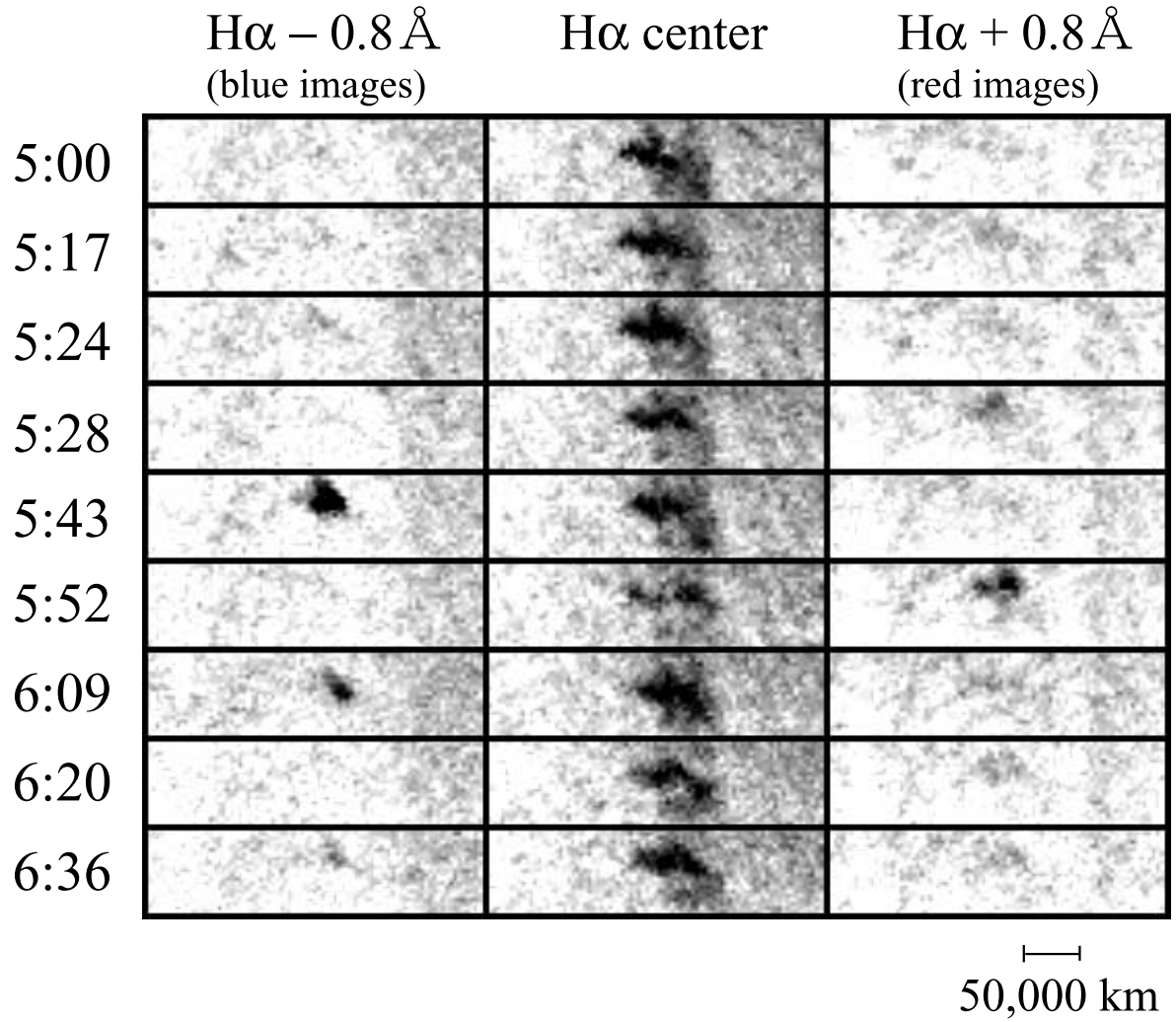

FIG. 7.—Hα images (Hα − 0.8 Å, *left*; Hα center; *middle*; and Hα + 0.8 Å, *right*) of an oscillating dark filament on 2001 April 10. The field of view is box P1 in Fig. 6. The filament started to oscillate at about 05:20 UT. The filament was seen in Hα + 0.8 Å at 05:28 UT, which means that it was undergoing downward motion, whereas it disappeared in the Hα + 0.8 Å image and appeared in the Hα − 0.8 Å at 05:43 UT, indicating that it was undergoing upward motion at 05:43 UT.

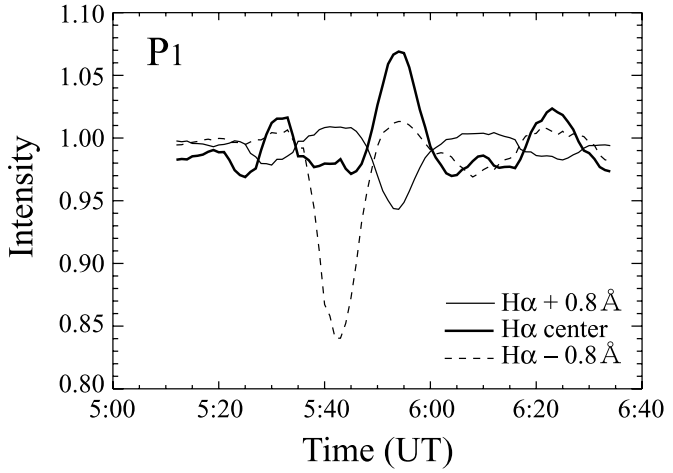

FIG. 8.—Time evolution of the emission of the filament in box P1 in Fig. 6. Thick line is the intensity in Hα center. The thin and dashed lines indicate the intensity in Hα + 0.8 Å and in Hα − 0.8 Å, respectively. The horizontal axis is time and the vertical axis is the intensity, normalized to that at 05:00 UT in each wavelength. Considering the alternate fluctuation of the intensity in Hα + 0.8 Å and Hα − 0.8 Å, we conclude that this filament oscillates.

wave on 2000 June 15 may be the coronal counterpart of the Moreton wave, while it is doubtful that the one on 2002 October 4 is the same wave as the Moreton wave. Hence, we cannot conclude that EIT waves are the same waves as Moreton waves. To make sure of this, we need higher cadence data from EIT.

As for the oscillating filament event, it is interesting that filament oscillations were caused only by an EIT wave. Many oscillating filaments have been studied, and we know various periods and motions of filaments. The period of one oscillation (in box P1 in Fig. 6) is about 28 minutes, which is similar to the 20 minute periods of flare-initiated filament oscillations (Ramsey & Smith 1965). On the other hand, this oscillation is different from the usual oscillations of quiescent prominences, which have periods of about 4 minutes (Tsubaki & Takeuchi 1986), or long-period line-of-sight velocity oscillations, which have 42–90 minute periods (Oliver & Ballester 2002). Jing et al. (2003) reported the periodic motion, which had a period of 80 minutes, along a solar filament initiated by a subflare, but neither the motion nor the period resembles those of our event at all. Eto et al. (2002) reported that a Moreton wave was the trigger of an oscillating filament, or a winking

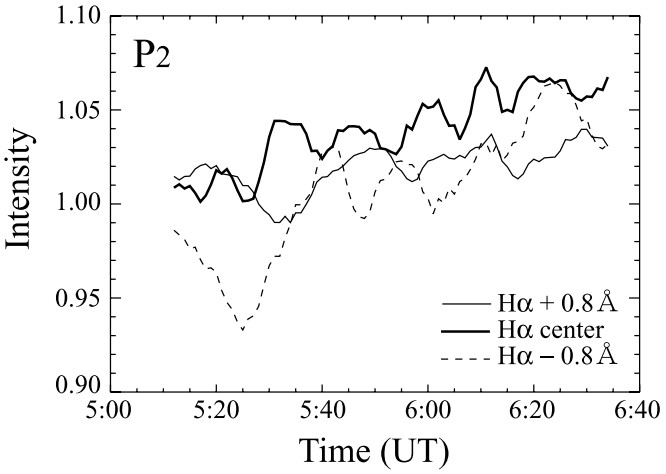

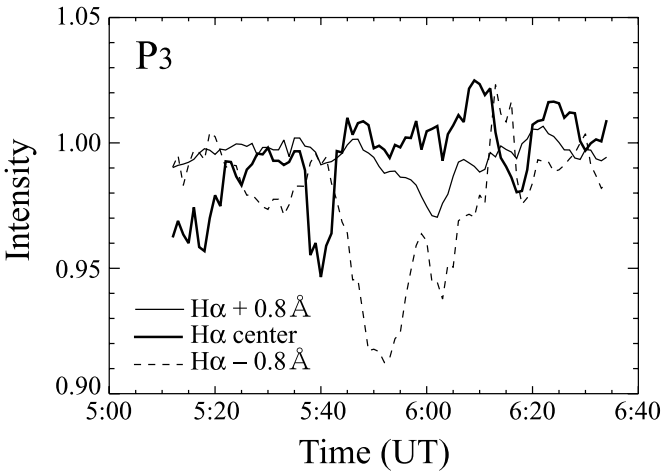

FIG. 9.—Same as Fig. 8, but for circles P2 and P3 in Fig. 6. These properties of lines are a little different from those of a winking filament, but these filaments are influenced by something like an EIT wave.

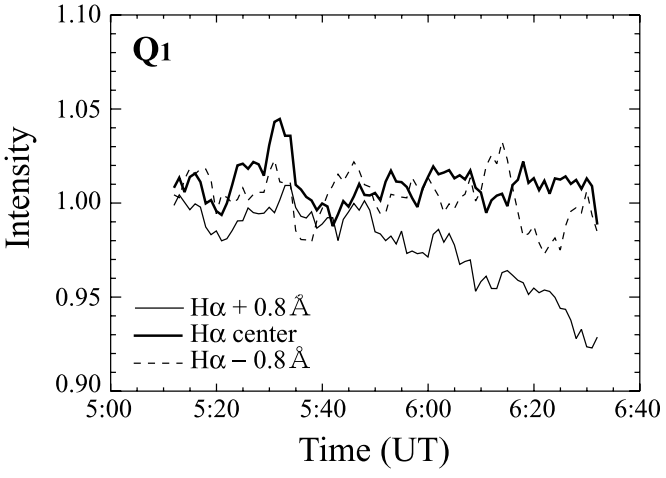

FIG. 10.—Time evolution of the emission of a dark filament that has no oscillation.

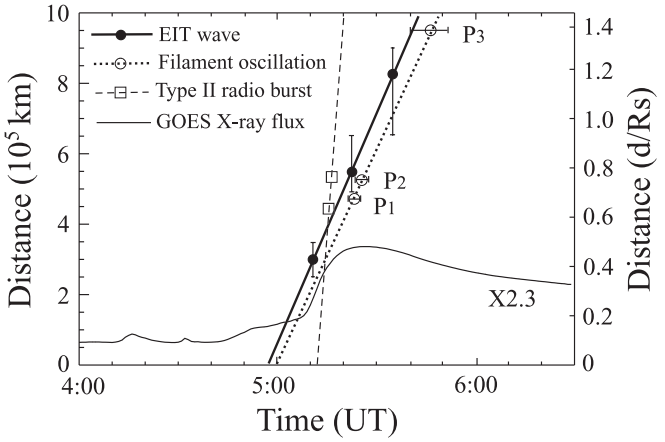

FIG. 11.—Time evolution of the distances of the EIT wave, the type II radio burst, and the filament oscillations. *GOES* X-ray flux data from the 1–8 Å channel are also shown. The distances from the flare site are plotted for the EIT wave and the filament oscillations, and the distance from the photosphere is shown for the type II radio burst. Rs represents the solar radius (695,800 km).

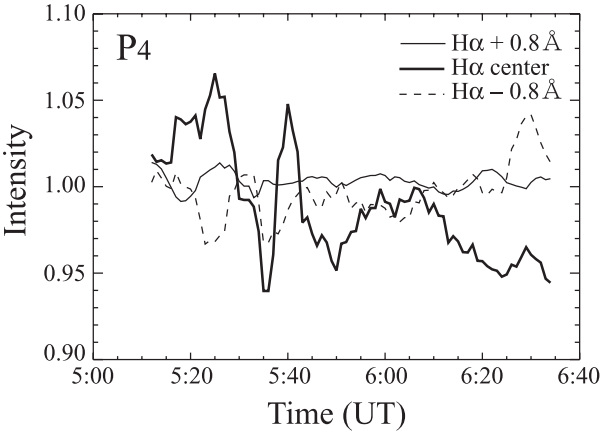

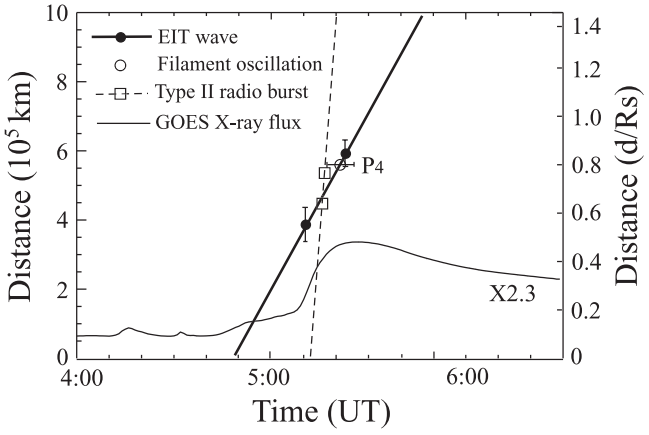

FIG. 12.—Same as Fig. 8 (*top*) and Fig. 11 (*bottom*), but for circle P4 in Fig. 6.

filament, while our event did not have a Moreton wave. It is not until now that an EIT wave has led an oscillating filament and we understand that EIT waves can have the same property as Moreton waves. However, a filament does not always oscillate even if an EIT wave passes over it. The Sun on 2001 April 10 had many filaments (Fig. 6), but we do not find any to oscillate except four filaments.

What is an EIT wave? With numerical simulations, Chen et al. (2002) suggested the relationship between Moreton and EIT waves. The legs of a piston-driven shock produce Moreton waves, while simultaneously a slower moving wavelike structure corresponds to the observed EIT waves. The observations reported by Harra & Sterling (2003) and Foley et al. (2003) are consistent with the model. It would be interesting to study whether the Chen et al. (2002) model can explain filament oscillations.

The authors thank T. Oda, P. F. Chen, S. Eto, H. Isobe, A. Asai, T. T. Ishii, and M. Kadota for useful discussions and the referee for helpful comments. *SOHO* is a mission of international cooperation between the European Space Agency and NASA. This CME catalog is generated and maintained by NASA and The Catholic University of America in cooperation with the Naval Research Laboratory. *SOHO* is a project of international cooperation between ESA and NASA. This work was supported in part by the JSPS Japan-UK Cooperation Science Program (principal investigators K. Shibata and N. O. Weiss).

REFERENCES

Asai, A., Ishii, T. T., Kurokawa, H., Yokoyama, T., & Shimojo, M. 2003, ApJ, 586, 624
Biesecker, D. A., Myers, D. C., Thompson, B. J., Hammer, D. M., & Vourlidas, A. 2002, ApJ, 569, 1009
Brueckner, G. E., et al. 1995, Sol. Phys., 162, 357
Chen, P. F., Wu, S. T., Shibata, K., & Fang, C. 2002, ApJ, 572, L99
Delaboudinière, J.-P., et al. 1995, Sol. Phys., 162, 291
Eto, S., et al. 2002, PASJ, 54, 481
Foley, C. R., Harra, L. K., Matthews, S. A., Culhane, J. L., & Kitai, R. 2003, A&A, 399, 749
Harra, L. K., & Sterling, A. C. 2003, ApJ, 587, 429
Hudson, H. S., Khan, J. I., Lemen, J. R., Nitta, N. V., & Uchida, Y. 2003, Sol. Phys., 212, 121
Jing, J., Lee, J., Spirock, T. J., Xu, Y., Wang, H., & Choe, G. S. 2003, ApJ, 584, L103
Khan, J. I., & Aurass, H. 2002, A&A, 383, 1018
Khan, J. I., & Hudson, H. S. 2000, Geophys. Res. Lett., 27, 1083
Kondo, T., Isobe, T., Igi, S., Watari, S., & Tokumaru, M. 1995, J. Commun. Res. Lab., 42, 111
Kurokawa, H., et al. 1995, Geomagn. Geoelectr., 47, 1043
Mann, G., Jansen, F., MacDowall, R. J., Kaiser, M. L., & Stone, R. G. 1999, A&A, 348, 614
Moreton, G. E. 1960, AJ, 65, 494
Narukage, N., Hudson, H. S., Morimoto, T., Akiyama, S., Kitai, R., Kurokawa, H., & Shibata, K. 2002, ApJ, 572, L109
Oliver, R., & Ballester, J. L. 2002, Sol. Phys., 206, 45
Pike, C. D., & Mason, H. E. 2002, Sol. Phys., 206, 359
Ramsey, H. E., & Smith, S. F. 1965, AJ, 71, 197
Smith, S. F., & Harvey, K. L. 1971, in Physics of the Solar Corona, ed. C. J. Macris (Dordrecht: Reidel), 156
Smith, S. F., & Ramsey, H. E. 1964, Z. Astrophys., 60, 1
Thompson, B. J., Reynolds, B., Aurass, H., Gopalswamy, N., Gurman, J. B., Hudson, H. S., Martin, S. F., & St. Cyr, O. C. 2000, Sol. Phys., 193, 161
Thompson, B. J., et al. 1999, ApJ, 517, L151
Tsubaki, T., & Takeuchi, A. 1986, Sol. Phys., 104, 313
Tsuneta, S., et al. 1991, Sol. Phys., 136, 37
Uchida, Y. 1968, Sol. Phys., 4, 30
———. 1974, Sol. Phys., 39, 431
Vršnak, B., Warmuth, A., Brajša, R., & Hanslmeier, A. 2002, A&A, 394, 299
Warmuth, A., Vršnak, B., Aurass, H., & Hanslmeier, A. 2001, ApJ, 560, L105